Observations and Modeling of Ionospheric Disturbances Triggered by Rockets

*Charles Lin[1], Chia-Hung Chen[1], Mitsuru Matsumura[2], Jia-Ting Lin[1]

1.Department of Earth Science, National Cheng Kung University, 2.National Institute of Polar Research, Research Organization of Information and Systems

This study presents two-dimensional structure of disturbances wave signatures in ionospheric electron density resulting from the rocket transit using the rate of change of the total electron content (TEC) derived from ground-based GPS receivers around Japan and Taiwan. From the TEC maps constructed for the recent five rocket launches around East Asia region, features of the V-shape shock wave fronts in TEC perturbations are prominently seen. These fronts, with period of 100-600 sec, produced by the propulsive blasts of the rockets appear immediately and then propagate perpendicular outward from the rocket trajectory with supersonic velocities between 800-1200 m/s for both events. Following the initial shock wave feature, various disturbances waves in TEC are seen. Twenty minutes after the rocket transits, delayed electron density perturbation waves propagating along the bow wave direction appear with phase velocities of 800-1200 m/s. According to the propagation character, these delayed waves may be generated by rocket exhaust plumes at earlier rocket locations at lower altitudes. The upward propagating disturbance waves due to exhaust plumes from lower altitude are also reconstructed by comprehensive model calculations.

Keywords: Ionospheric Disturbance Waves, Rocket Exhaust

Study of dynamics of tsunami ionospheric hole from geomagnetic observation

*Yuto Tomida[1], Tatsuya Kanaya[1], Masashi Kamogawa[1], Makoto Uyeshima[2]

1.Department of Physics, Tokyo Gakugei University, 2.Earthquake Research Institute, The University of Tokyo

Approximately several minutes after the occurrence of the mainshock of the M9.0 off the Pacific coast of Tohoku Earthquake on 11 March 2011, various geo-electromagnetic phenomena was in Japan and even in the magnetic conjugate point of Japan (i.e. Australia) through magnetic field lines as a field align current. In this paper, we show electromagnetic phenomena after the 2011Tohoku earthquake in the ionosphere such as tsunami ionospheric hole, seismo-field align current, Rayleigh-wave-induced ionospheric arc current, and seimic- ionospheric ring current (SRIC). SRIC was highly related to tsunami ionospheric hole observed by GPS-TEC.

Keywords: Magnetic field, Earthquake, Tsunami, Tsunami ionospheric hole

Smal-scale variations of ionospheric TEC observed with a hyper-dense GNSS receiver network

Yuji Takeda[1], Naoki Ito[1], *Toshitaka Tsuda[1], Atsuki Shinbori[1]

1.Research Institute for Sustainable Humanosphere

We employ the GNSS meteorology to estimate TEC (total electron content) and PWV (Precipitable Water Vapor) in the ionosphere and troposphere, respectively, from the propagation delay of GNSS signal. We established a hyper-dense GNSS receiver network in Uji using 7 to 15 receivers with 1-2 km spacing. We found difference of PWV in 10 km was 3-10 mm during a heavy rain. For a future system, we use inexpensive single-frequency (SF) receivers. Because SF receiver cannot eliminate the ionospheric delay, we interpolate the delay referring to the results from nearby dual frequency (DF) receivers.
We investigated ionospheric delay by the Uji network, taking advantages of QZSS(Quasi-Zenith Satellite System) that gives signals at high elevation angles. Effects of ionospheric perturbations due to sun-rise/sun-set and a geomagnetic storm were small, so they do not give serious influence on PWV. During a travelling ionospheric disturbance, a wavy structure with a horizontal scale of several tens km was recognized. These ionospheric effects can be compensated by a linear or quadratic interpolation.
We corrected the ionospheric delay on SF observation with 30 sec sampling with SEID developed by GFZ. The resulting error of PWV compared with DF solution was about 1.50 mm in RMS. By improving the time resolution of the interpolation from 30 to 1sec, error is suppressed by about 70%.

Keywords: GNSS meteorology, hyper-dense GNSS receiver netwrok , PWV (precipitable water vapor), TEC (total electron content), ionospheric propagation delay

Observation of mid-latitude sporadic E over North America by GNSS-TEC

*Takato Suzuki[1], Masato Furuya[2], Kosuke Heki[2], Jun MAEDA[3]

1.Hokkaido University, 2.Faculty of Science, Hokkaido University, 3.Hokkaido University Library

Maeda and Heki. (2014) succeeded in capturing sporadic E (Es) over Japan two-dimensionally, using the observation of Global Navigation Satellite System - Total Electron Content (GNSS-TEC). We aimed to capture Es over the western coast of North America where there is mid-latitude same as Japan and GNSS stations are dense.
First, we chose the dates whose critucal frequencies of Es (foEs) were more than 12 MHz at Disisonde in Pt. Arguello (lat: 34.8, lon: 239.5) in the morning and noon in 2006 through 2015 from May to August. Second, we made GNSS-TEC maps.
We succeeded in capturing Es over America and indicated that a strong Es appeared also at different longitude can be captured by GNSS-TEC. Es observed this time had E-W direction slope. It is though that this reflects E-W wind shear.

Keywords: Sporadic E, GNSS-TEC

Generating mechanism of Medium-Scale Traveling Ionospheric Disturbance using a GPS network in Alaska

Takuya Mizoguchi[1], *Yuichi Otsuka[1], Kazuo Shiokawa[1], Michi Nishioka[2], Takuya Tsugawa[2]

1.Institute for Space-Earth Environmental Research, Nagoya University, 2.National Institute of Information and Communications Technology

In our previous study, using global positioning system (GPS) data taken from GPS receivers in Alaska in 2012 and in Northern Europe in 2008, we investigated two-dimensional maps of total electron content (TEC) perturbations with a time resolution of 30-s and a spatial resolution of 80 km80 km in longitude and latitude to disclose statistical characteristics of Medium-Scale Traveling Ionospheric Disturbance (MSTID) at high-latitudes. Based on the statistical characteristics of MSTID at high-latitudes, we have found that the observed MSTIDs are divided into three groups: 1. daytime MSTID occurring in winter in Alaska and Northern Europe, 2. nighttime MSTID occurring in summer in Northern Europe, and 3. dusk MSTID occurring in winter in Alaska. The daytime and nighttime MSTIDs at high-latitudes are consistent with those observed at mid-latitudes in terms of local time dependence of their occurrence rate and propagation direction, but the dusk MSTID has not been observed at mid-latitudes. In this presentation, we focus on the generation mechanisms of the dusk MSTID which occurs in winter in Alaska by investigating whether the MSTID is generated by the same mechanism as those at mid-latitudes, from the view point of electrodynamics and neutral atmosphere dynamics.
At first, we consider the generation mechanisms of MSTIDs from a standpoint of electrodynamics. We find that vertical component of plasma motion is restricted and amplitude of TEC perturbation by $E \times B$ drift is small because magnetic field line is close to vertical at high-latitudes. We discuss the theory that polarization electric fields in sporadic E layer play an important role in generating that MSTID through E- and F-region coupling process. According to this theory, MSTID occurs simultaneously at conjugate points in the northern and southern hemisphere connected by geomagnetic field lines. However, the observational results show that local time dependence of MSTID in Alaska and New Zealand is different. Therefore, we conclude that MSTID observed dusk in winter in Alaska could not be generated by electrodynamics.
Secondly, we research whether the dusk MSTID is generated by atmospheric gravity waves (AGWs) or not. Previous studies suggest that MSTIDs could be caused by AGWs excited by auroral activities. In this study, we have investigated various indicators which could represent auroral activity, such as ROTI (Rate of TEC change Index), AE index and Kp index. We have found that there is no clear correlation between occurrence rate of MSTID and these indices.
To determine the location of the AGW sources, we apply the backward ray tracing method of AGWs. Results of a backward ray tracing analysis show that the AGWs can reach ionosphere from an altitude of 10 km in 24 of 34 events. In a few cases, AGWs traced backward from the ionosphere reach a critical level at an altitude of the stratosphere. This result indicates a possibility that AGWs excited by polar vortex in the stratosphere propagate to the ionosphere and generate the MSTIDs. We need further studies about source region of AGWs to reveal generation mechanisms of MSTIDs at high-latitudes.

Keywords: ionosphere, traveling ionospheric disturbance, GPS

Spectral analyses of resonance scattering of Sr and Ba for determination of thermospheric neutral wind

*ko saito[1], Yoshihiro Kakinami[1], Masa-yuki Yamamoto[1]

1.Kochi Uniersity of Technology

1. Introduction: We developed a measurement technique for the wind velocity profile in the thermospheric rarefied atmosphere by Lithium(Li) releases from sounding rockets in cooperation with JAXA and NASA. We observed barium (Ba) and barium ion (Ba^+) released by sounding rocket in Norway in November, 2014, and observed the thermospheric neutral wind and the ion drift at an altitude range of 150~400 km. In the future, Japan is going to carry out the similar measurement using strontium (Sr), and the experiment using the Sr ejection system was performed as a preliminary experiment on ground in Gunma prefecture in September, 2014. Here we report both of the results of the spectrum analyses from the observed images of Sr and Ba in order to verify the released components of Ba and Sr.

2. Spectrum analysis: The spectrum observation method of this experiment in Norway was observation of spectrum images by a camera (Nikon D700) with an attached diffraction grating (500 line/mm) without a slit to the front of lens. The spectrum observation for the Sr preliminary experiment on ground was performed using a video camera (SONY DCR-PC101) attached to the same diffraction grating with a slit as well as a fiber input type spectrophotometer. We analysed the brightness distribution of the 1st order spectrum section using a developed image processing software by using IDL (Interactive Data Language) language and made a brightness level in each pixel on the image. Then, photographed bright-line spectrum of the Ar gas by a small Ar discharge tube was used for calibration of the spectrum camera and the spectrum video camera. The Ar lines are used as a basis of wavelengths for calibration. We acquired multiple Ar line wavelengths to calibrate calibrated the brightness spectrum distribution of Sr emission on ground as well as Ba and Ba^+ resonance scattering light in thermosphere. In addition, the spatial integrated spectrum strength obtained by the fiber input type spectrophotometer was also used for Sr measurement.

3. Spectrum analysis and discussion: From the spectrum analysis of the images taken at the rocket experiment in Norway, emission spectrum of wavelengths at 455 nm, 557 nm and 610 nm - 661 nm was confirmed. The wavelengths were fixed as the wavelengths of the documented Ba^+ and the Ba emissions at 455 nm and 553 nm. From the spectrum analysis, we can confirm an emission wavelength at 460 nm obtained at the Sr ground experiment as 460.7 nm emission which is documented as the Sr spectrum line. We could clearly detect Sr 460.7 nm by integrating multiple spectrum sections on an image. From the data analysis for the spectrophotometer measurement, we confirmed a spectrum of iron (Fe) and aluminum (Al) at 635 nm, 644 nm and 656-659 nm as well as oxygen (O_2) at of 668 nm –671 nm, suggesting the effect by the thermite reaction in case of the Sr release.

4. Conclusion: We confirmed the emissions at the of wavelengths 455 nm and 557 nm from the sequential spectrum images which the sounding rocket experiment in Norway provided and those were fixed as Ba^+ and Ba, thus Ba release and ionization were confirmed. In addition, it is concluded that when we confirm a brightness peak at 460.7 nm by the two types of spectrum data obtaind by the ground measurement, Sr release and emission was confirmed.

Keywords: strontium, resonance scattering, thermosphere

Numerical simulation of magnetic field variation associated with equatorial plasma bubble

*Tatsuhiro Yokoyama[1], Claudia Stolle[2]

1.National Institute of Information and Communications Technology, 2.GeoForschungsZentrum Potsdam, Germany

Equatorial plasma bubble (EPB) is a well-known phenomenon in the equatorial ionospheric F region. As it causes severe scintillation in the amplitude and phase of radio signals, it is important to understand and forecast the occurrence of EPB from a space weather point of view. The development of EPB is known as a evolution of the generalized Rayleigh-Taylor instability. We have developed a new 3D high-resolution bubble (HIRB) model for EPB and presented nonlinear growth of EPB which shows very turbulent internal structures such as bifurcation and pinching. Recently, it has been reported that high-resolution magnetometer onboard low Earth orbit satellites such as CHAMP and Swarm can detect small-scale magnetic field perturbation associated with EPBs. It is interpreted as the diamagnetic effect produced by pressure gradient-driven current, and field-aligned current flowing along the walls of EPBs. We have upgraded the 3D numerical simulation model by removing the equipotential magnetic field assumption so that 3D current distribution can be calculated. The magnetic field variations produced by the current associated with EPBs are consistent with the in situ observations and expected physical models. It is also important for internal magnetic field modeling because such magnetic field variations are comparable to that of the lithospheric contribution.

Keywords: plasma bubble, magnetic field, simulation, CHAMP satellite

Preliminary report of a sounding rocket experiment to elucidate electron heating in the Sq current focus
- Observations of DC Electric field and VLF band plasma wave -

*Yuka Ataka[1], Keigo Ishisaka[1], Takumi Abe[2], Makoto Tanaka[3], Atsushi Kumamoto[4], Akimasa Yoshikawa[5], Hiroki Matsushita[5]

1.Toyama Pref. Univ., 2.ISAS/JAXA, 3.Tokai Univ., 4.Tohoku Univ., 5.Kyushu Univ.

The Sq current system occurs in the lower ionosphere in the winter daytime. The center region of the Sq current system is appeared the specific plasma phenomenon such as electron heating, strong electron density disturbance. S-310-44 sounding rocket equipped with each scientific instrument and is launched toward the center of the Sq current system. The rocket observe the physical quantity for the investigation of the specific phenomenon. As similar experiment, S-310-37 sounding rocket had been performed in the past, however it was not possible to observe the electric field component of the magnetic field-aligned direction. It is one of the reasons that the photo electron caused by the sunlight that is irradiated to the rocket body, and affect the electric field observations. It is very difficult to remove the influence of the photo electron from the observed data. If it is possible to put the electrode of the electric field sensor outside of the region where there become the photo electron around the rocket body, the influence of the photo electron can be reduced. Therefore, the antennas need a length as long as possible to observe the electric field. Accordingly, the antennas of S-310-44 sounding rocket is 4m tip-to-tip that is twice as length than the antennas of S-310-37 sounding rocket. The purpose is to reduce the influence of the photo electron moreover to measure the electric field more accuracy.
It was carried out the S-310-44 sounding rocket experiment at Uchinoura Space Center (USC) at 12:00 LT on January 15, 2016. This rocket passed through near the center of the Sq current system. In addition, scientific observation instruments that are equipped on the rocket also operated normally. In Electric Field Detector (EFD), the antennas have started extension after 67 seconds (altitude 81km) from launch. After 81 seconds (altitude 97km) the full extension, the observation was started. There was not seen the effect by photo electron in observed the electric field data. Here we analyze the electric field data obtained in the S-310-44 sounding rocket. And we describe the derivation result of the electric field that it is important for the investigation of the Sq current system generating mechanism.

Keywords: electric field , sounding rocket experiment, Sq current system

Sounding rocket experiment to clarify electron heating phenomena in the Sq current focus - Plasma wave observation -

*Atsushi Kumamoto[1], Keigo Ishisaka[2], Yuka Ataka[2], Takao Takahashi[3], Makoto Tanaka[3], Takumi Abe[4]

1.Department of Geophysics, Graduate School of Science, Tohoku University, 2.Toyama Prefectural University, 3.Tokai University, 4.JAXA

In order to clarify electron heating phenomena in the center of Sq current focus in the winter ionosphere, the sounding rocket experiment S-310-44 was launched at 21:00 UT (12:00 JST) on January 15, 2016 at Uchinoura Space Center (USC). Plasma Wave Monitor (PWM) onboard the S-210-44 was successfully measured plasma waves in a frequency range from 300 Hz to 22 MHz along the rocket trajectory with apex altitude of 160 km, which is also confirmed to be near the Sq current focus by using data from magnetometer chain on the ground. The AC electric field was picked up with two antenna elements (EFD-ANT-1 and 2), and respectively amplified by two preamplifiers (EFD-Pre-1 and 2) of the Electric Field Detector (EFD). Then, two signals were fed to two PWM inputs (PWM-HF and PWM-VLF), respectively. The signal fed to PWM-HF was sampled at 81.92 MSPS and converted to spectrum in a frequency range from 20 kHz to 22 MHz with 400 frequency steps. The signal to PWM-VLF was sampled at 81.92 kSPS and converted to spectrum in a frequency range from 300 Hz to 20kHz with 400 frequency steps. These spectra were obtained every 125 msec. EFD antenna elements were stored on the ground and deployed at altitude of 85 km. So the altitude range from 85 km to 160 km are covered in ascent, and all altitude range below 160 km are covered in descent.
During the flight, the following phenomena were identified: (1) Harmonic emissions of lower hybrid resonance (LHR) were found in a frequency range from several hundred Hz to several kHz. Their frequencies changes depending on the ambient plasma density and likely on the ion compositions. They are enhanced at altitude around 100 km in ascent but not enhanced at the same altitude in descent. (2) Upper hybrid resonance (UHR) waves were not found in a frequency range around several MHz. In most previous sounding rocket experiment, UHR waves were found in altitude range higher than 200 km, and masked at altitude below 200 km by the artificial radio waves from the ground. In this experiment, the artificial radio waves were not so intense to mask the other emissions.
The LHR waves can be generated by various energy inputs. Baker et al. [2000] reported that LHR emissions were found in the sounding rocket experiment, and suggested that they are caused by the whistler waves from the thunderstorms on the ground. The enhancement of LHR only in ascent suggests that the energy source of LHR wave is localized in narrow area in E region of the ionosphere. Through the comparisons with data from the other instruments onboard the S-310-44 such as electron density and temperature (FLP), DC and AC electric fields (EFD), and currents (MGF), we will be able to discuss the energy source of the observed LHR waves in more detail.

Keywords: The sounding rocket experiment S-310-44, Sq current focus, Plasma wave observation, Lower hybrid resonance wave

Preliminary report of a sounding rocket experiment to elucidate electron heating in the Sq current focus
- Observations of thermal electron energy distribution -

*Takumi Abe[1], Keigo Ishisaka[2], Atsushi Kumamoto[3], Makoto Tanaka[4], Takao Takahashi[4], Hiroki Matsushita[5], Akimasa Yoshikawa[5]

1.Japan Aerospace Exploration Agency Institute of Space and Astronautical Science Department of Solar System Sciences, 2.Toyama Prefectual University, 3.Tohoku University, 4.Tokai University, 5.Kyushu University, Faculty of Sciences

Sounding rocket observations in Japan suggest that the electron temperature profile occasionally exhibits the local increase by several hundred K at 100-110 km altitudes at 1100-1200 LT in winter. Detailed study of the temperature profiles indicates that such an increase is closely related to the existence of Sq current focus, because it becomes more significant when the measurement is made near the center of Sq focus. In order to understand a general feature and to investigate a generation mechanism of this unusual phenomena, a sounding rocket experiment was carried out.
In this experiment, “S-310-44” rocket equipped with a suite of five science instruments was launched from Uchinoura Space Center at 12:00 JST on January 16, 2016 after being convinced that the Sq current was approaching to the planned rocket trajectory. In this presentation, we will focus on the energy distribution of thermal electrons and electron temperature obtained from FLP (Fast Langmuir Probe) instrument onboard the rocket.
In the FLP instrument, a small AC voltage with a frequency of 2 kHz was superimposed on a triangular voltage bias with an amplitude of 3 V. It is possible to estimate energy distribution from the amplitude of the second harmonic component of 2 kHz in the probe current. Moreover, the electron temperature can be estimated from the electron energy distribution, when the energy distribution is considered to be *Maxwellian*. Another function of the FLP is to be able to provide a small-scale (< 1 m) electron density perturbation, which can be estimated from the electron saturation current provided by a fixed bias spherical probe installed on the rocket axis.
During this experiment, a group of Kyushu University has continuously measured the geomagnetic field on the ground to estimate exact position of Sq current focus, because it is required for the rocket trajectory to be close enough to the current focus. Their analysis about the magnetometer data suggests that *in-situ* observations of electrons, magnetic and electric fields were conducted in the distance of 200 to 300 km from the current focus.
The FLP successfully made its measurement during both upleg and downleg of the rocket flight. Observations of the energy distribution suggest that the electron temperature increased by about 200 K with respect to the background in the altitude range from 100 to 110 km. It is also significant that the observed energy distribution unlikely seems *Maxwellian* distribution and sometimes exhibits a possible existence of *non-Maxwellian* component in the high electron temperature region. Power spectrum analysis of the electron current by the fixed bias probe indicates that the amplitude in the frequency range of several hundred Hz increased at the E region altitude. In particular, it is remarkable that the strong electron density perturbation was observed in the broad frequency range at altitudes from 95 to 110 km. In this presentation, we give a report on the preliminary analysis of the thermal electron measurements in more detail.

Keywords: Sq current system, sounding rocket, electron heating

Variation of equivalent current system representing geomagnetic Sq variation in the period of 1980-2010

*Masahiko Takeda[1]

1.Data Analysis Center for Geomagnetism and Space Magnetism, Graduate School of Science, Kyoto University

Spherical harmonics analysis was performed for the geomagnetic Sq field from 1980 to 2010 for every universal hour on each day. Solar activity dependence of the total Sq currents was confirmed, and variation in each solar cycle was also reflected in the total current intensity.
More detailed features of the long trend of the Sq field will be discussed in the presentation.

Keywords: geomagnetic daily variation,, equivalent current system, secular variation, solar activity

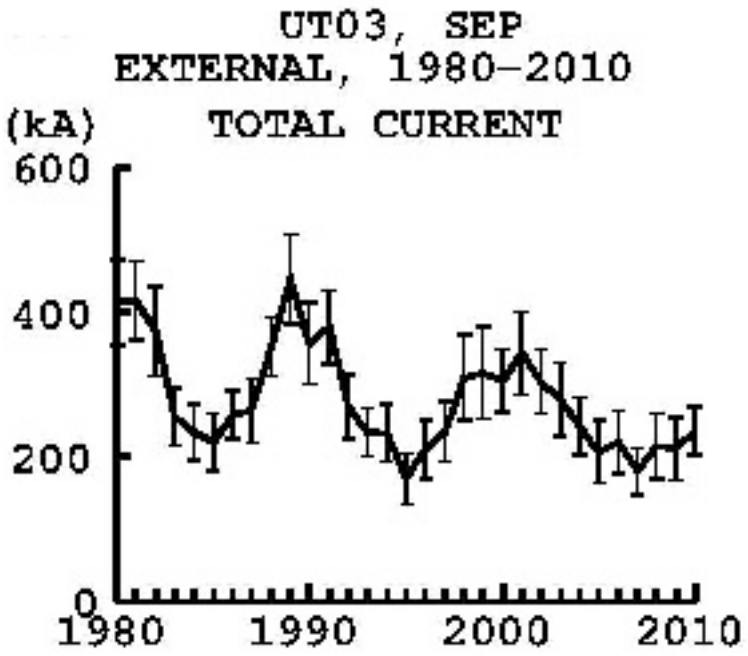

Horizontal Distributions of Sprites and the Relation to Parent Lightning Discharges Derived from JEM-GLIMS Nadir Observations

*Mitsuteru Sato[1], Toru Adachi[2], Tsuyoshi Sato[3], Tomoo Ushio[4], Takeshi Morimoto[5], Makoto Suzuki[6], Atsushi Yamazaki[6], Yukihiro Takahashi[1]

1.Faculty of Science, Hokkaido University, 2.Meteorological Research Institute, 3.Department of Cosmosciences, Hokkaido University, 4.Graduate School of Engineering, Osaka University, 5.Faculty of Science and Engineering, Kinki University, 6.ISAS/JAXA

JEM-GLIMS carried out ~3-years nadir observations of lightning discharges and lightning-producing transient luminous events (TLEs) at the ISS. In this period, JEM-GLIMS succeeded in detecting 8357 lightning events and 699 TLEs. From the detailed data analyses, 42 and 508 events in 699 TLEs are confirmed to be sprites and elves, respectively. It is found that the delay time of the sprite occurrence from the parent lightning occurrence is ~1 ms in all the sprite events (i.e., short-delayed sprites) and that the sprite emissions occurred above the parent lightning emissions. However, the exact location of the sprite emissions was slightly displaced from the peak location of the parent lightning emissions, which is regarded as the return stroke point. We statistically estimated the displacement and found that the median and average values are 13.6 km and 13.3 km, respectively. This result is consistent with the pervious report of *Lu et al.* [JGR, 2013], who suggested that the short-delayed sprites tend to occur within 30 km from the return stroke point. At the presentation, we will show the characteristics of the horizontal distributions of sprites and discuss the possible mechanism of the displacement more in detail.

Keywords: Lightning, TLEs, ISS

Lower-thermospheric wind variations in auroral patches during the substorm recovery phase

*Shin-ichiro Oyama[1], Kazuo Shiokawa[1], Yoshizumi Miyoshi[1], Keisuke Hosokawa[2], Brenton J Watkins[3], Junichi Kurihara[4], Takuo T. Tsuda[2], Christopher T Fallen[3]

1.Institute for Space-Earth Environmental Research, Nagoya University, 2.University of Electro-Communications, 3.Geophysical Institute, University of Alaska Fairbanks, 4.Hokkaido University

Responses of the polar thermosphere and ionosphere to geomagnetic substorms have been widely investigated by many researchers. Representative mechanisms that may cause such variations are thermal energy dissipation by the Joule and particle heating processes and momentum transfer by the Lorentz force. The mechanisms and thermospheric/ionospheric responses have been studied by analyzing data mainly at the expansion phase or around the substorm onset. In contrast the substorm recovery phase has had little focus for most researchers. A motivation for this work is spontaneous and dramatically large variations of density, temperature, and dynamics in the thermosphere and ionosphere at the substorm recovery phase.
At the substorm recovery phase, measurements of the lower-thermospheric wind with a Fabry-Perot interferometer (FPI) at Tromsø, Norway found the largest wind variations in a night during appearance of the auroral patches. Taking into account magnetospheric substorm evolution of plasma energy accumulation and release, the largest wind amplitude at the recovery phase is a fascinating result because it is generally assumed that the energy dissipation at the recovery phase is smaller than that at expansion phase and onset. The results are the first detailed investigation of the magnetosphere-ionosphere-thermosphere coupled system at the substorm recovery phase using comprehensive data sets of solar wind, geomagnetic field, auroral pattern, and FPI-derived wind. This study used three events in November 2010 and January 2012, particularly focusing on the wind signatures associated with the auroral morphology, and found three specific features: (1) wind fluctuations that were isolated at the edge and/or in the darker area of an auroral patch with the largest vertical amplitude up to about 20 m/s and with the longest oscillation period about 10 minutes, (2) when the convection electric field was smaller than 15 mV/m, and (3) wind fluctuations that were accompanied by pulsating aurora. This approach suggests that the energy dissipation to produce the wind fluctuations is localized in the auroral pattern. Effects of the altitudinal variation in the volume emission rate were investigated to evaluate the instrumental artifact due to vertical wind shear. The small electric field values suggest weak contributions of the Joule heating and Lorentz force processes in wind fluctuations. Other unknown mechanisms may play a principal role at the recovery phase.

Keywords: aurora, thermosphere, Fabry-Perot interferometer, substorm recovery phase

Test observations by a frequency-tunable resonance scattering lidar

*Mitsumu K. Ejiri[1], Takanori Nishiyama[1], Takuo T. Tsuda[2], Makoto Abo[4], Katsuhiko Tsuno[3], Satoshi Wada[3], Takayo Ogawa[3], Takuya Kawahara[5], Takuji Nakamura[1]

1.National Institute of Polar Research, 2.The University of Electro-Communications, 3.RIKEN, 4.Graduate School of System Design, Tokyo Metropolitan University, 5.Faculty of Engineering, Shinshu University

The National Institute of Polar Research (NIPR) is leading a six year prioritized project of the Antarctic research observations since 2010. One of the sub-project is entitled the global environmental change revealed through the Antarctic middle and upper atmosphere. Profiling dynamical parameters such as temperature and wind, as well as minor constituents is the key component of observations in this project, together with a long term observations using existent various instruments in Syowa, the Antarctica (69S). As a part of the sub-project, we are developing a new resonance lidar system with multiple wavelengths and plan to install and operate it at Syowa, Antarctica. The lidar will observe temperature profiles and variations of minor constituents such as Fe, K, Ca^+, and aurorally excited N_2^+. The lidar system is being developed with trial and error in test observations of the metal atom and ion density and the MLT temperature profiles. The lidar will be installed at Syowa in Antarctica by the 58th Japan Antarctic Research Expedition (JARE 58). In this presentation, we will report current status of the system developments and discuss results of the test observations.

Keywords: resonance scattering lidar, Mesosphere Lower-Thermosphere Region, Temperature measurement, Metal atom, Metal ion

One night variation of horizontal phase velocity distribution of mesospheric gravity waves at Syowa

*Takashi S. Matsuda[2,1], Takuji Nakamura[1,2], Masaki Tsutsumi[1,2], Mitsumu K. Ejiri[1,2], Yoshihiro Tomikawa[1,2]

1.National Institute of Polar Research, 2.Graduate University for Advanced Studies

Gravity waves, generated in the lower atmosphere, can propagate to the mesosphere and the lower thermosphere, and transport great amount of energy and momentum, and release them at various altitude regions. Among many parameters to characterize gravity waves, horizontal phase velocity is very important to discuss vertical propagation and where the momentum is released. Near the mesopause region, OH and other airglow imaging has been used for investigating the horizontal structures of gravity waves for more than two decades. Although the huge amount of the image data has been observed at various observation sites all over the world, a time consuming manual procedure has been used for extracting horizontal propagation characteristics from airglow data. This causes difficulty in obtaining a global map of gravity wave characteristics in the mesopause region. Another important fact on the mesospheric gravity wave studies is that observations over the Antarctic region were quite rare despites a significant amount of gravity waves generated in this region.
Matsuda et al., 2014 developed new statistical analysis method for deriving horizontal phase velocity spectrum of gravity waves derived from airglow imaging data. It is suitable to not only deal with a large amount of data, but also reveal temporal variation of phase velocity spectrum. In this study, we obtained 9 horizontal phase velocity spectra every an hour at 1501-0000 on May 11 2013 at Syowa (69S, 40E). We compared these spectra with background wind using re-analysis data (MERRA) and MF radar data, and found that effect of wind filtering by critical level could not explain the temporal variation.

Keywords: Atmospheric gravity waves, Airglow imaging, Mesosphere

Long-term variation of horizontal phase velocity spectrum of mesospheric gravity waves observed by an airglow imager at Shigaraki : Comparison with tropospheric re-analysis data

*Daiki Takeo[1], Kazuo Shiokawa[1], Hatsuki Fujinami[1], Yuichi Otsuka[1], Takashi S. Matsuda[2], Mitsumu K. Ejiri[2], Takuji Nakamura[2], Mamoru Yamamoto[3]

1.Institute for Space-Earth Environmental Research Nagoya University, 2.National Institute of Polar Research, 3.Research Institute for Sustainable Humanosphere, Kyoto University

Atmospheric gravity waves (AGWs) generated in the lower atmosphere transport momentum into the upper atmosphere and release it when they break near the mesopause region. The released momentum drives global-scale pole-to-pole circulation in the upper atmosphere, causing global mass transport. The AGW propagation and its momentum transport depend on horizontal phase velocity of AGWs. There were many studies about the AGWs in the past by using radars, lidars and airglow imagers, and various AGW parameters such as wavelengths and phase velocities were studied. However, long-term (>10 years) variation of horizontal phase velocity spectrum of the mesospheric small-scale AGWs, which can be measured by airglow imagers, has not been studied yet.
In this study, we analyze the horizontal phase velocity spectrum of AGWs by using mesospheric 557.7-nm airglow images obtained at Shigaraki MU Observatory (34.8 deg N, 136.1 deg E) of Kyoto University over ~17 years from October 1, 1998 to July 26, 2015. We use 3-dimensional Fourier analysis procedures of airglow images proposed by Matsuda et al. (JGR, 2014), making it possible to analyze large amount of data.
Seasonal variations of propagation direction of AGWs was clearly identified (Spring : North-East and South-West, Summer : North-East, Fall : North-West, Winter : South-West). Several longer-term variations of direction / intensity were identified for each season with a time scale of several years. The power spectrum density of horizontal phase velocity changes with 7-8 years timescale in winter and 2-3 years in spring.
The east-west anisotropy (summer: eastward, winter: westward) of AGW propagation is probably caused by filtering of gravity waves due to mesospheric jet (summer: westward, winter: eastward) (e.g., Nakamura et al., EPS, 1999; Ejiri et al., JGR, 2003). However, north-south anisotropy (summer: northward, winter: southward) cannot be explained by mesospheric jet. Then we investigate the location of possible AGW sources relative to Shigaraki by using tropospheric re-analysis data about vertical flow velocity to understand the north-south anisotropy. There are regions of strong vertical velocities at south of Japan due to the Baiu seasonal rain front during summer and at north-east of Japan due to wintry low pressure during winter. Thus we consider that the north-south anisotropy of AGW propagation direction is due to the location of AGW sources in summer and winter.
Next, we investigated the relationships of longer-term variations of power spectrum density (PSD) of horizontal phase velocity of AGWs with tropospheric re-analysis data, NINO index, AO index and sunspot numbers particularly for summer and winter. There is a correlation between longer-term variations of PSD and tropospheric re-analysis data at south of Japan during summer and north-east of Japan during winter. These regions nearly correspond to the rain front in summer and the wintry low pressure in winter, as we described before. Thus we think more certainly that the north-south anisotropy of AGW propagation direction is controlled by the relative location of AGW sources. We could not find any clear correlations of PSD variations with NINO index, AO index and sunspot numbers.

Keywords: mesospheric gravity waves, horizontal phase velocity spectrum, long-term analysis, airglow imager, tropospheric re-analysis data

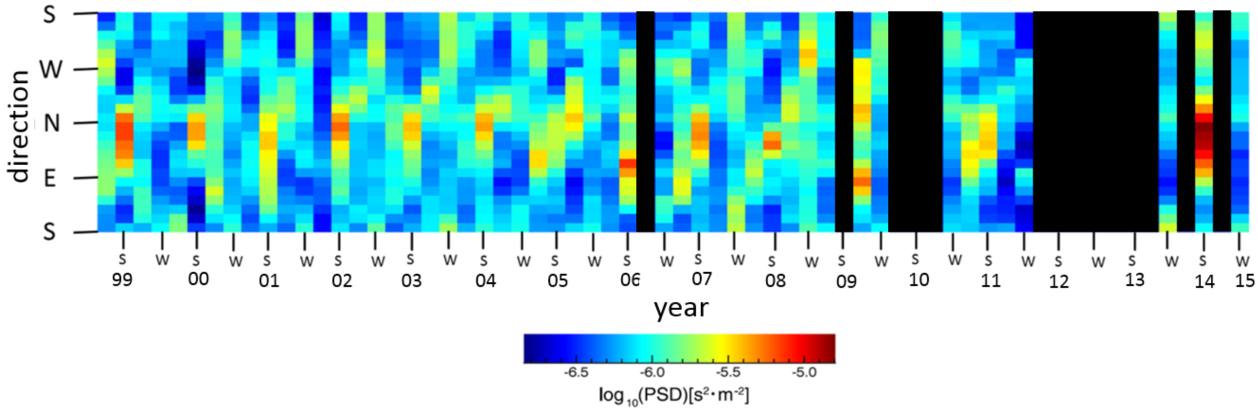

Variations in the reflection height in the lower ionosphere associated with typhoons using LF transmitter signals

*Hiroyo Ohya[1], Keisuke Asada[2], Fuminori Tsuchiya[3], Kazuo Shiokawa[4], Hiroyuki Nakata[1], Kozo Yamashita[5], Yukihiro Takahashi[6]

1.Graduate School of Engineering, Chiba University, 2.Faculty of Engineering, Chiba University, 3.PPARC, Graduate School of Science, Tohoku University , 4.Institute for Space-Earth Environmental Research, Nagoya University, 5.Department of Electrical Engineering, Salesian Polytechnic, 6.Graduate School of Science, Hokkaido University

So far, several studies for gravity waves caused by typhoons have been reported, although there are few studies for the lower ionosphere variations associated with typhoons using LF transmitter signals. In this study, we investigate variations of the D-region height associated with a typhoon of 11-20 June, 2012 using phase data of LF transmitter signals. There were two magnetic storms (minimum Dst values:-51 nT on 12 June and -71 nT on 17 June) in these dates. The propagation paths were Fukushima-Pontianak (PTK, Indonesia, 40 kHz) and Saga-PTK (60 kHz). We converted the phase data to reflection heights based on Earth-ionosphere waveguide mode theory. The period of the reflection height variations was analyzed by wavelet transform. The reference days were 23, 24, and 29 June, 2012, which were also geomagnetically quiet days. We excluded the periods of the reflection height variations seen in these reference days from the periods during the typhoon. In daytime during the typhoon, several solar flares were identified by the GOES X-ray flux. When the solar flares occurred, the reflection heights were largely decreased. Only nighttime data of the reflection height were analyzed because the duration of the gravity waves is expected to be several hours. As a result, the common periods of the reflection height over both propagation paths were 45.3 minutes on 15 June, 2012, and 76.1 minutes on 16 June. The duration of the periods was about 50 minutes in nighttime. In the two nights, medium-scale traveling ionospheric disturbances were not observed in the GPS-TEC data over Japan. The horizontal wavelengths were calculated from the onset time difference of the oscillations between the two propagation paths, and difference of the distance between the source location (the typhoon) and the two propagation paths. The horizontal wavelengths were estimated to be 483 -662 km for the 45.3 minutes and 1222 -1346 km for the 76.1 minutes. The horizontal wavelengths were comparable or longer than previous studies.

Development of VLF/LF field strength prediction program using wave-hop theory

*Kenro Nozaki[1], Kuniyasu Imamura[1], Shigeru Tsuchiya[1], Kitauchi Hideaki[2]

1.National Institute of Information and Communications Technology, 2.Kitauchi Lab.

A numerical calculation program for VLF/LF radio wave field strength by means of wave-hop theory adopting the recommendations of the International Telecommunication Union Radiocommunications Sector (ITU-R). The electric field at the receiving point consists of a ground wave and sky waves of from 1-hop to 10-hop modes reflected between the ground and bottom of the ionosphere. Parameters at every ground and ionospheric reflection point are calculated for given day, time, transmitting power, transmitting/receiving location within 16000km. A detailed calculation algorithm and some characteristic results are presented.

Keywords: VLF/LF, field strength, wave-hop theory

Basic development of direction finding system for lightning discharge at small balloon

*Masaaki Yoshinaga[1], Masa-yuki Yamamoto[1]

1.Kochi University of Technology

1. Introduction
As for the observation of the upper atmosphere, new observation technique has been born with a technological change in history. Balloon observation is lower-cost than other upper atmospheric observation technique like rockets, and in the recent years various experiment is performed with large balloons of JAXA. In addition, in the recent years when the downsizing of microcontrollers and the sensors has been realized rapidly, the observing experiment using small weather balloons is currently becoming feasible for the university laboratory level [1,2].
In this study, we developed the basics of balloon borne type small thunder direction-finding payload system. At present, the Meteorological Agency thunder reporting are leading the thunder observation in Japan. General technique of the thunder observation includes ground station as well as satellites for weather observation. However, most of the observation via the altitude area that a thundercloud developed (approximately within 5km-10km) has not yet been performed. For that reason, here, we introduce a thunder observation system to be equipped on high-altitude small balloons for weather observation use, and it is thought that provided data by making in-site measurements might be useful scientifically. In this paper, we report a design and the experiment of the small discharge direction-finding system and a future view [3].
2. System development
We adopted an electromagnetic wave detection type system by using a small loop antenna with a simple structure for balloon deployment with the direction-finding technique aboard. The developed system consists of a SD memory card and a GPS receiver for the precise data acquisition, a pair of orthogonal loop antenna, pre-amplifier for signal amplification with bias circuit, and 2-channel A/D converters.
3. System evaluation experiment
We performed an experiment for confirming the electric discharge detectabilities by using a discharging tube as a microscopic thunder generator. Confirming if a small loop antenna of φ100 mm× 90 turns could detect the change of the magnetic field. The purpose of experiment was checking distance-dependency and declination-dependency of the loop antenna when changing the distance direction of the discharging tube as a electromagnetic wave source. The distances of 0.5 m, 0.7 m, 1.0 m and 1.2 m were used for confirming each electromagnetic wave strength.
In addition, for confirming declination-dependency of the crossed loop antennas, chopping angle of the loop antenna was charged from right to left to realize 0-90 degrees changes in the direction relations artificially.4. Experimental results and discussion
In the distance-dependency experiment, it was confirmed that a second multinomial relation between signal strength A and distance d. The reception signal was weak but it canbe said that we can detectthe electromagnetic waves from the discharging tube quantitatively. On the other hand, the direction finding was impossible due to the low characteristics of accepted sampling rate on the used micro-controller, signal delay between the both channels growing at a time of the A/D conversion with the mbed microcontroller.
5. Summary
The developed system perferms continuous data collection without any significant problems. Microscopic discharge experiment was used for simulating a thunderbolt in laboratory. However, we have never tried the outdoor setting of this system, thus the electro-magnetic wave detection

coming from nature a lightning was not yet confirmed. Downsizing of the system and performance experiment under the simulated environment of the upper atmosphere is necessary when we consider the real balloon deployment. There exist two kinds of electric discharge phenomena that the polarity of discharge is anode-related lightning and cathode-related one. Thus, it is necessary to build an additional dipole antenna for the real direction-finding.

Keywords: Thunder, Electromagnetic wave, Balloon

Development and evaluative flight experiment result of small high-altitude balloon system optimized for domestic operation

*Takamasa Hiratsuka[1], Hiroki Kono[1], Masa-yuki Yamamoto[1]

1.Kochi University of Technorogy

1.Introduction: Special high-altitude airplanes, sounding rockets and high-altitude balloons are used for observation technique in high-altitude area. High-altitude balloons have an advantage of making easy to product simple-structure payloads in comparison, therefore it has also an advantage of the cost per experiment when physical loads on the payload are small. In addition, high-altitude balloons are able to be launched slowly upward with a velocity of several m/s and do not use chemical reactions to provide lift-off, thus an advantageous technique in scientific observation. Applying these kind of advantages, the application of using weather balloons in high-altitude balloon experiment increased recently. Weather balloons are made of rubber that approximately 3 m in diameter, mounting payload weight is approximately 5 kg per balloon or less. In comparison with other observation techniques the small scale and low cost high-altitude balloon experiment may show the effectiveness in future when the weight of payload is not so heavy. Based on these backgrounds, the importance of the high-altitude balloon is greatly considered to escalate the role in high-altitude observation drastically depending on a way of the utilization. However, the observation technique using the small high-altitude balloons has not been spread in Japan rather than the continental countries mainly because ensuring safety of operation and recovery of the payload is difficult by geographical limitation in Japan. In this study, we are focusing on constructing operative system aboard the small high-altitude balloons that the development and inspection were possible at university laboratory level. We developed the controlled-descent-style payload technique using a small parafoil with automatic servocontrol to overcome the problem, and examined the validity of the developed system and utility through a performance evaluation experiments.
2. Developed airframe and low altitude flight experiment: We designed an examination airframe as is shown in figure to offer for various flight tests and conducted low altitude flight experiments by throwing down from a tower wagon an altitude of approximately 20 m, being controlled by remote console on ground.
3. Results of the experiment: The ratio of the gliding distance to the falling altitude was approximately 2 which we calculated from GPS position and barometer data recorded with a SD memory card. Long period flight is necessary for the evaluation with the stable gliding altitude of the parafoil, however, due to the short term evaluation period, obtaining the precise gliding ratio was difficult. Analizing the relationship between the heading orientation of the flight and the right and left servocontrol angles, it was confirmed that the state of airframe heading direction was changed from the east to the south when turning the servo controlled rudder with pulling down the right side arm.
4. Summary: Design validity of the developed airframe with the servocontrolled parafoil was confirmed by low altitude flight experiments. As for the future problem, it is necessary to evaluate with a flight from higher altitude, and to test it to confirm the ratio of the gliding distance to the falling altitude in the long-range flight. Assuming the more realistic large scale flight experiment in near future, we will develop a reliable bus apparatus and the balloon communication system to the ground stations. In addition, for the future mission, we have to confirm the design of mission and bus apparatus for the small balloon payload.

Keywords: small high-altitude balloon, parafoil, guidance control

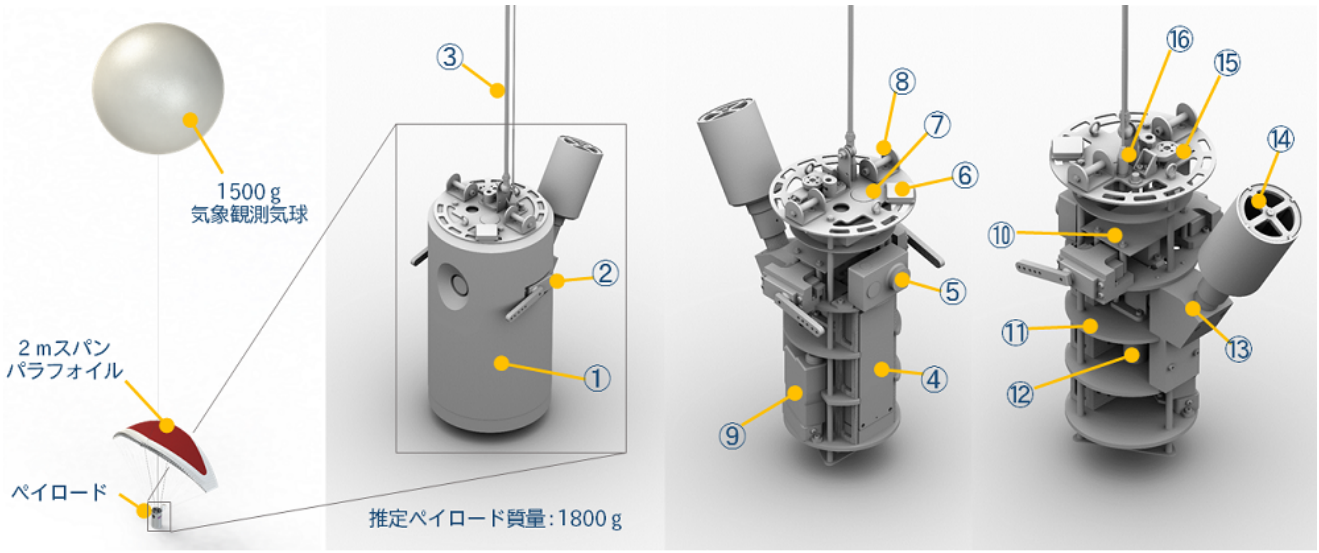

① 保護外装（発泡スチロール）
② RC サーボモーター
③ パラフォイル固定ロッド
④ Li-Poバッテリー（耐衝撃外装）
7.4 V / 7500 mAh
⑤ 水平方向カメラ
⑥ 外部GPSアンテナ
⑦ 垂直方向カメラ
⑧ パラフォイル締結金具
⑨ 430 MHz帯アマチュア無線機
⑩ Main Control Unit (MCU)
⑪ 内部構造板（MDF材）
⑫ 緊急パラシュート射出ボンベ
⑬ 空圧シリンダー
⑭ パラシュート格納容器
⑮ 気球切り離し機構
⑯ UHF帯アンテナ

Water vapor estimation using digital terrestrial broadcasting waves - Results using reflected waves -

*Seiji Kawamura[1], Hiroki Ohta[1], Hiroshi Hanado[1], Masayuki Yamamoto[1], Nobuyasu Shiga[1], Kouta Kido[1], Satoshi Yasuda[1], Tadahiro Goto[1], Ryuuichi Ichikawa[1], Jun Amagai[1], Kuniyasu Imamura[1], Miho Fujieda[1], Kentaro Ishizu[1], Hironori Iwai[1], Shigeo Sugitani[1]

1.National Institute of Information and Communications Technology

We, National Institute of Information and Communications Technology (NICT), are developing a water vapor measurement system using digital terrestrial broadcasting wave. One of our goals is to develop a 2D water vapor monitoring system with distributed many small receivers. Horizontal distribution of water vapor mopnitoring will be contribute to increase the precision of weather forecast with data assimilations. Very precise measurements (at least several tens of pico-second order) are needed for the effective observations. Phase fluctuations of local oscillators at radio tower and receivers are essential error factors. So we measure the propagation delay at two receiving points on the same line including the radio tower. Each result includes phase fluctuations of local oscillators at radio tower and receivers. Phase fluctuation of local oscillator at radio tower will be canceled out by taking the difference. We can estimate water vapor between two receiving points by synchronization between their local oscillators.
We are developing a real-time delay (phase of delay profiles) measurement system with software-defined radio technique. Each TV station has their own local oscillators. Out system is improved and it can measure phase fluctuations of radio waves from whatever TV station stably for a long time. We are planning a proving test for synchronization of local oscillators at different sites.
In this presentation we report a method and results of water vapor measurment without synchronization of local oscillators. We observe phase variations of digital terrestrial broadcasting waves at cartain site. If there is a reflector at the opposite side from the radio tower, we can observe direct waves and reflected waves simultaneously. Measurement is conducted using single local oscillator at the observing point. So we can measure a round trip propagation delay between the observing point and reflector without synchronization of local oscillators. NICT is located at about 29 km westward from the Skytree. A building is located at about 1 km westward from NICT. Both direct and reflected waves can be observed at NICT. We have a groundbase meteorological observatory equipment at NICT. Provagation delay can be calculated using these data on the assumption that these data are representative of the meteorological condition around there (within 1 km). Observed time vriations of propagation delay using digital terrestrial broadcasting waves correspond to the calculation.

Keywords: digital terrestrial broadcasting wave, water vapor

Global occurrence distributions and rates of lightning and TLEs and their LT dependences

*Tsuyoshi Sato[1], Mitsuteru Sato[2], Tomoo Ushio[3], Takeshi Morimoto[4], Toru Adachi[5], Makoto Suzuki[6], Atsushi Yamazaki[6], Yukihiro Takahashi[1]

1.Department of Cosmosciences, Graduate School of Science, Hokkaido University, 2.Department of Cosmoscience, Hokkaido University, 3.Information and communication engineering department, Osaka University, 4.Faculty of Science and Engineering, Kindai University, 5.The Meteorological Satellite and Observation System Department, Meteorological Research Institute, 6.Institute for Space and Astronautical Sciences, Japan Aerospace Exploration Agency

Transient Luminous Events (TLEs) are the instantaneous discharge phenomena excited by intense cloud-to-ground (CG) discharges. Using the optical data obtained by the FORMOSAT-2/ISUAL data, global occurrence distributions and rates of TLEs were estimated. However, due to the sun-synchronous polar orbit of the FORMOSAT-2 satellite, the local time (LT) dependences of the global occurrence rates of TLEs has not been estimated. In this study, we analyzed optical data obtained by the JEM-GLIMS (Global Lightning and Sprite Measurements on JEM-EF) instruments onboard the ISS (International Space Station) for the period from December 2012 to November 2014. Since the orbital inclination of the ISS is 51°, we can estimate more accurate global occurrence distributions and rates of lightning and TLEs and their LT dependences. From our data analyses, it is found that the estimated occurrence distributions of lightning and TLEs are mainly centered over the Africa, Southeast Asia, and Central America. It is also found that the LT dependences of lightning and TLEs occurrence rates showed small peak at 20LT and gradual increase from 00LT to 03LT. At the presentation, we will show the results derived from our data analyses more in detail and will discuss the possible reasons for the estimated LT dependences of lightning and TLEs occurrence rates.

Keywords: TLEs

Study of atmospheric gravity waves of orographic origin by airglow imaging

*Masahiro Okuda[1], Hidehiko Suzuki[1]

1.Meiji Univ.

Excitation and propagation processes of atmospheric gravity waves (AGWs) have been widely studied by both an observation and modeling schemes to understand energy and momentum balance in the middle atmosphere. Major sources of AGWs are known to be an interaction between winds and topography like mountains, inhomogeneous thermal absorption due to lands and sea distribution, active convections in troposphere, and wind shears etc. In particular, AGWs with orographic origin is thought as one of the important factors for a seasonal variation in mesospheric circulation, since the source is fixed to the ground. An airglow imaging system for OH7-3 band is newly developed and installed in Kawasaki, Japan (35.6°N, 139.5°E) in Nov 2015 to investigate propagation and excitation mechanisms of mountain waves over the Kanto plain. Since Kanto Plain is sandwiched by mountain rich area including Mt. Fuji and the Pacific Ocean, identification of AGWs from orographic origin is expected to be easy. For example, continuous easterly wind in a surface level would excite mountain waves with zero ground phase speed over the Kanto plain. In addition, a simple shape of cross section (i.e. Model-like shape) of the source (Mt. Fuji) would make comparison with modeling studies easy. In this talk, details of the airglow imaging system and prompt results from early observations are presented.

Keywords: Atmospheric gravity wave, Middle atmosphere, Mountain wave

Investigation on Na layer response to geomagnetic activities using resonance scatter measurement by Odin/OSIRIS

*Takuo T. Tsuda[1], Takuji Nakamura[2], Mitsumu K. Ejiri[2], Takanori Nishiyama[2], Keisuke Hosokawa[1], Toru Takahashi[1], Jörg Gumbel[3], Jonas Hedin[3]

1.The University of Electro-Communications, 2.National Institute of Polar Research, 3.Stockholm University

The Na layer is normally distributed from 80 to 110 km, and the height range is corresponding to the ionospheric D and E region. In the polar region, the energetic particles precipitating from the magnetosphere can often penetrate into the E region and even into the D region. Thus, the influence of the energetic particles to the Na layer is one of interests in the aspect of the atmospheric composition change accompanied with the auroral activity.
There are several previous studies in this issue. For example, recently, we have reported an initial result on a clear relationship between the electron density increase (due to the energetic particles) and the Na density decrease from observational data sets obtained by Na lidar, EISCAT VHF radar, and optical instruments at Tromsoe, Norway on 24-25 January 2012. However, all of the previous studies had been carried out based on case studies by ground-based lidar observations.
In this study, we have performed, for the first time, statistical analysis using Na density data from 2004 to 2009 obtained with the Optical Spectrograph and InfraRed Imager System (OSIRIS) onboard Odin satellite. In the presentation, we will show relationship between the Na density and geomagnetic activities, and its latitudinal variation. Based on these results, the Na layer response to the energetic particles will be discussed.

Keywords: Na layer, energetic particle, Odin/OSIRIS

Performance evaluation of low-cost airglow camera for mesospheric gravity wave measurements -Part 3: Image processing

*Shin Suzuki[1]

1.Faculty of Regional Policy, Aichi University

Atmospheric gravity waves significantly contribute to the wind/thermal balances in the mesosphere and lower thermosphere (MLT) through their vertical transport of horizontal momentum. It has been reported that the gravity wave momentum flux preferentially associated with the scale of the waves; the momentum fluxes of the waves with a horizontal scale of 10-100 km are particularly significant. Airglow imaging is a useful technique to observe two-dimensional structure of small-scale (<100 km) gravity waves in the MLT region and has been used to investigate global behavior of the waves. Recent studies with simultaneous/multiple airglow cameras have derived spatial extent of the MLT waves. Such network imaging observations are advantageous to ever better understanding of coupling between the lower and upper atmosphere via gravity waves. In this study, we newly developed low-cost airglow cameras to enlarge the airglow imaging network. Each of the cameras has a fish-eye lens with a 185-deg field-of-view and equipped with a CCD video camera (WATEC WAT-910HX) ; the camera is small (W35.5 x H36.0 x D63.5 mm) and inexpensive, much more than the airglow camera used for the existing ground-based network (Optical Mesosphere Thermosphere Imagers (OMTI) operated by Solar-Terrestrial Environmental Laboratory, Nagoya University), and has a CCD sensor with 768 x 494 pixels that is highly sensitive enough to detect the mesospheric OH airglow emission perturbations. In this presentation, we will report some results of performance evaluation using the data obtained during test observations made at Shigaraki, Japan, in 2014.

A numerical study on decrease of electron temperature inside the sporadic E layer

*Yumika Sakamoto[1], Takumi Abe[2], Wataru Miyake[1]

1.Department of Aeronautics and Astronautics Graduate School of Engineering, Tokai University, 2.Institute of Space and Astronautical Science, Japan Aerospace Exploration Agency

The sporadic E (Es) layer has been studied for a long time. Wind-shear theory is generally accepted about its generation mechanism. This theory explains an accumulation process of the electron density, but hardly gives information on thermal energy budget inside the layer.Although the electron temperature is the parameter for discussing the thermal energy budget inthe ionosphere, there were few data of reliable electron temperature in the Es layer in the past.Thus, few information on the electron temperature are only available, and there were very few discussions about the thermal energy budget inside the Es layer.The sounding rocket "S-520-29" was launched from Uchinoura Space Center at 19:10 JST on August 17, 2014. The purpose of this experiment is to elucidate spatial structure of the Es layer in the lower ionosphere.Langmuir probe installed on this rocket is capable of making high-speed sampling of probe current, and thereby it is possible to estimate the electron temperature and density more than 10 samples per second. In addition, it becomes possible to obtain the temperature and density in shorter time interval by adopting a new method of interpolation for obtained current -voltage relationship. Data calculated by using such an interpolation based on Langmuir probe measurements suggest that the electron temperature significantly decreased inside the Es layer with respect to the background temperature. Furthermore, the detailed trend of the electron temperature from its boundary toward the center of Es layer was revealed due to the interpolation.In this study, we will discuss a physical implication of the observed high electron temperaturefor energy budget inside the Es layer by conducting numerical calculation in which we consider electrons, ions, and neutrals in the vertical 1-D direction. The electron temperature distribution is estimated for various conditions of electron density using electron energy equation.The photoelectron heating and Joule heating are included in the calculation as a heating process, and the electrons' interaction with the neutrals and the ions is considered as a cooling process. It was found that the electron temperature tends to decrease inside the Es layer when the electron density becomes significantly larger as in the Es layer. Furthermore, we tried to find an important process dominant for the electron temperature increase by examining adependence of various parameters such as ion density and the electric field. We will present a result from this numerical consideration.

Keywords: Sounding rocket, sporadic E layer

Derivation of cross-section shape of sporadic E by HF-Doppler spectral analysis

*Hiroki Ohta[1], Ichiro Tomizawa[1]

1.Center for Space Science and Radio Engineering ,UEC

The surface of the frontal sporadic E (Es) was not same cylindrical shape, but was found that had the structure that varied according to the arrival place on the cross-section surface [1] [2].
In this study, surface of cross-section of the frontal Es via the middle reflection point of HFD of Kanto is observed and three dimensions of details data of the electric field strength every the Doppler shift frequency of the neighborhood at the midway point passage time is demanded. the change is considered to be the incidence angle dependence of the equivalence of value dispersion cross section when an electric wave was incident on a surface of slim frontal Es from the lower part in time for field strength that cut and brought down these data every constant frequency. Because the baseline halfway houses between each transmission and reception points are different, the section of the reflection surface of the frontal Es is estimated finely. A movement direction and the speed of the frontal Es is found by performing this analysis at a plural observation point and the cross-section of the reflection surface of the whole surface of the frontal Es is derived in detail.
For this method, the result that investigated a cross-section structure of the shape of surface of the frontal Es lower part by analyzing HF Doppler spectral using four transmit frequencies in detail at multiple receiving points of the Kanto HFD observation network was showed. A change really demands an average change from the electric field strength graph which cut and brought down observation data in the frequency direction by a quadratic equation fitting by the least-squares method because it is difficult to greatly analyze it directly. Based on this average change, the max field intensity, the time and 3 dB time width every the Doppler shift frequency are found. The surface of cross-section width of the surface of the frontal Es undersurface is found from the product of width and the horizontal mobility speed with the irregularity of the surface of cross-section is estimated at 3 dB time width from the max field intensity and the time.
The above-mentioned method of analysis was applied, found it about a sectional structure of surface of the frontal Es observed in 21 JST(UT+9) of January 16, 2013 and 19th in detail. The surface of the frontal Es of January 16 was 205 m/s and move to the 279° direction, January 19 was 151 m/s and move to the 205° direction. The both of frontal Es were high speed and have small cross-section width. The high speed frontal Es has few changes at peak field intensity for time, and has the structure that was cylindrical or near. In addition, as for the surface of the frontal Es of January 16, section width of high frequency becomes about the same with Fresnel zone diameter (4.1km); center of circle structure becoming higher leading electron density in this at the midway point passage time of the Es at each frequency was different, and center sectional structure knew that there was a degree of leaning.
By the lecture, I am going to argue about the sectional structure by applying this analytical method for the different surface of the water-formed Es of the Doppler shift change curve.

[1] Hiroki Ohta and Ichiro Tomizawa: Derivation of shape of cross-section of frontal sporadic E by the HF Doppler spectral analysis, JPGU 2015, P-EM27-P11, 2015.5.
[2] Ichiro Tomizawa and Kotaro Fujii: HF propagation model reflected by frontal Es, JPGU 2013, PEM29-01, 2013.5.

Keywords: ionosphere, sporadic E, HF Doppler shift observation

Possible shear instability in the daytime midlatitude sporadic-E observed with InSAR and GPS-TEC

*Jun MAEDA[1], Takato Suzuki[1], Masato Furuya[1], Kosuke Heki[1]

1.Hokkaido University

Small-scale horizontal structures of daytime midlatitude sporadic E are studied by interferometric synthetic aperture radar (InSAR) and GPS total electron content (TEC) observations over Japan. With GPS-TEC observations, sporadic E with foEs higher than 16 MHz can be detected [Maeda and Heki, 2014]. A dense array of GPS receiving stations in Japan (GEONET) enables us to image horizontal shapes of sporadic E by plotting vertical TEC anomalies on a map. Such TEC maps revealed that sporadic E over Japan has a common shape which is elongated in the east-west (E-W) direction with typical length and width of ~200 km and ~20 km, respectively, regardless of occurrence latitudes [Maeda and Heki, 2014; 2015]. In this study, we observed smaller-scale structures by InSAR as well as GPS-TEC observations. The spatial resolution is ~300 m for InSAR and ~2 km for GPS-TEC (by analyzing raw slant TEC time series).
The results show that small-scale plasma patches are embedded in large scale frontal structures and such small patches are quasi-periodically located both in zonal and meridional directions.
There are two major candidates for the generation mechanism of daytime sporadic E structure, i.e, namely, atmospheric gravity waves, and the Kelvin-Helmholtz (K-H) instability. We speculate that the K-H instability in the neutral atmosphere under the presence of vertical shear of zonal winds would create billow structures elongated in the zonal direction. On the other hand, secondary instability, such as secondary turbulance in the neutral atmosphere or gradient-drift instability are the two major possible drivers for the patch structuring in the meridional direction.

Keywords: sporadic-E, InSAR, GPS-TEC

Estimation of electron density distribution of strong Es using VOR, AIS and Ionosonde and its application to the VHF interference model of long-distance propagation wave

*Takuya Nitta[1], Ichiro Tomizawa[1], Atsushi Yamamoto[2], Shinji Saitoh[3]

1.Center for Space Science and Radio Engineering, UEC, 2.Japan Coast Guard Academy, 3.Electronic Navigation Research Institute

The University of Electro-Communications observe Very High Frequency Electric wave Reflected in Sporadic E layer in Chofu and Kure[1].It is necessary to check electronic density structure over a wide area to expect intervention of the VHF data transmission system (GBAS - VDB) long-distance propagating wave of GBAS by Strong Es[2]. Regional structure of sporadic E (Es) and transport property have become clear by Yanagisawa's study[3], but it isn't done clearly yet about the electron density distribution structure of Es. Es propagation model of ITU - R was guaranteed only to frequency 80 MHz by ionospheric reflection attenuation Γbased on a Es transmission observation in 1960 's and the correspondence system with ionosonde vertical critical frequency foEs around the middle specular point[4],[5]. But the distance between the middle specular point and ionosonde could confirm the correspondence with Es propagation model of ITU - R for the first time in case of about 400 km in the range in 2013-VOR long-distance transmission observation around the 110 MHz in 2015.Using this relation, result of presumption of electron density distribution structure from a lot of VOR reception electric power was compared with electron density distribution from AIS, Yamagawa, Okinawa ionosonde.
Yamagawa (31.20N, 130.62E) and Okinawa (26.68N, 128.15E) observed Es in the East China Sea, Okinawa and around the Kyushu south where the distance with ionosonde will be about 400 km in the range at 10-JST time 15:00 on June 15, 2014. It could be confirmed that Es has moved to about 330 deg direction by high 108 km and speed about 70 m/s. This Es showed that the electron density the strong Es territory where 1.0 x 10^13 el/m^3 appeared, and which can put electron density in Okinawa ionosonde is parallel with strong Es where 9.2 x 10^12 el/m^3 mostly in the Okinawa south and around the east around 10:10-11:30 in AIS. In case of this time’s Es, it was assumed that there was a possibility beyond the VOR reception electric power-98dBm that intervention with VOR and GBAS - VDB is worried about when Es propagation model of ITU - R was applied. An analysis sample by this way will be indicated in the lecture, and I report on a relation between the distribution of the electron density, the feature of the transport property and intervention occurrence of strong Es conversantly.
Reference
[1] Yamahata Takuya, Ichiro Tomizawa and Atsushi Yamamoto: Wide area Es structure observation system development by VHF area long-distance transmission reception, SGEPSS, B005-P038, 2012.
[2] Shinji Saito, Ichiro Tomizawa and Atsushi Yamamoto: Influential consideration of VOR long-distance transmission by sporadic E to GBAS –VDB, science technical report, vol. 114, SANE2014-125, pp113-118, 2015.
[3]Shinya Yanagisawa: Strong regional structure of sporadic E and study of transport property by VHF area long-distance propagating wave observation, UEC Master thesis, 2016.
[4] K. Miya and T. Sasaki: Characteristics of ionospheric Es propagation and calculation of Es signal strength, *Radio Sci.*, vol.1, pp.99-108, 1966.
[5] ITU-R:Recommendation of ITU-R, Method for calculating sporadic-E field strength, Rec.ITU-R P.534-4,1999.

Small-scale magnetic fluctuations of lower atmospheric origin as observed by low Earth orbit satellites ~ Identification of lower atmospheric phenomena ~

*Tadashi Aoyama[1], Toshihiko Iyemori[1], Kunihito Nakanishi[1]

1.Graduate School of Science, Kyoto University

We recently found small-scale (0.1~5 nT) magnetic fluctuations above the ionosphere in middle and low latitudes with period about 20-30 sec along the satellite orbit observed by the low Earth orbit satellites such as the CHAMP (2000~2009) or the SWARM (2013~) having precise magnetometer (resolution: 0.065 nT). We name these magnetic fluctuations the "Magnetic Ripples" (MRs). The magnetic fluctuations are perpendicular to geomagnetic main field. By comparing the magnetic fluctuations observed by two SWARM satellites at the same latitude, we could confirm that they are the manifestation of the spatial structure of small scale field-aligned currents along the satellite orbit. The amplitude of the MRs have local time, geographical and seasonal dependence, therefore we suppose that localized field-aligned currents are generated by the ionospheric E-layer dynamo driven by the atmospheric gravity waves propagated from lower atmosphere. Typhoons and volcanic eruptions are known to generate gravity waves, and we report the characteristic of the MRs probably generated by a volcanic eruption, typhoons, rain fronts etc.. We try to identify the lower atmospheric phenomena which cause the MRs.

Keywords: ionospheric dynamo, field-aligned current, acoustic resonance, SWARM, CHAMP, magnetic ripple

Ionospheric Hole made by the Kwangmyongsong-4 Rocket Launched from Norh Korea on Feb. 7, 2016, and Increase of Thrust of its Second Stage Engine

*Kosuke Heki[1], Yuki Nakashima[2], Liming He[1]

1.Department of Earth and Planetary Sciences, Faculty of Science, Hokkaido University, 2.Department of Natural History Sciences, Graduate School of Science, Hokkaido University

Exhaust gas from ascending rockets and ballistic missiles bring large amount of water molecule to the ionosphere. Such water molecules receive positive electric charges from atmospheric ions, and their dissociative recombination with ionospheric electrons causes the formation of ionospheric holes (region of low electron density). Ionospheric total electron content (TEC) can be measured by comparing the carrier phases of the two L-band signals from Global Navigation Satellite System (GNSS) satellites, and such GNSS-TEC technique is useful in studying such ionospheric holes (Furuya & Heki, 2008). By analyzing the GNSS data from the dense network of GNSS receivers in Japan (GEONET), Ozeki & Heki (2010) compared ionospheric signatures by the two ballistic missiles launched from eastern North Korea, i.e. the 1998 Taepodong-1 and the 2009 Taepodong-2, and inferred their difference in thrusts. In 2012 December, a rocket, Unha-3, was launched southward from a launch pad in northwestern part of North Korea, and Nakashima & Heki (2014) studied the ionospheric hole made above the Yellow Sea/the South China Sea by the second/third stage engine of the rocket using a GLONASS (the Russian GNSS) satellite.

On February 7th, 2016, a new rocket Kwangmyongsong-4, was launched southward from the same launch pad at 9:31 JST (0:31 UT), and succeeded in putting an earth-observing satellite (KMS-4) into orbit. Here we studied the ionospheric hole made by this launch. Unlike the previous case, we could detect clear hole signatures with multiple satellites of both GPS and GLONASS. The hole emerged at 6-7 minutes after the launch, and its position and emergence time were similar to the previous 2012 case. However, the areal extent and the amount of TEC decrease were much more in the 2016 case. In the attached figure, we compare the TEC time series observed with GPS Satellite 29 from GEONET stations in western Kyushu, together with the past three cases. Clearly, the TEC decreases in the 2016 case are much larger than the past cases.

In all the rocket (missile) launches from North Korea, the first stage engine did not reach the ionospheric height, and it was the second stage engine that made the ionospheric holes (Ozeki & Heki, 2010). The overall figure of the present Kwangmyongsong-4 rocket looks quite similar to the previous Unha-3, but its payload (satellite) is suggested to be larger in size than the 2012 case. The thrust of the second stage engine may have been made more powerful to put this relatively large satellite into orbit. However, the vertical TEC above the Yellow Sea in the present case was ~30 TECU, which is twice as large as in the 2012 launch, and the comparison of the thrust in the two cases may need a more quantitative discussion.

References

Furuya, T. and K. Heki, Ionospheric hole behind an ascending rocket observed with a dense GPS array, Earth Planets Space, 60, 235-239, 2008.

Nakashima, Y. and K. Heki, Ionospheric hole made by the 2012 North Korean rocket observed with a dense GNSS array in Japan, Radio Sci., 49, doi:10.1002/2014RS005413, 2014.

Ozeki, M. and K. Heki, Ionospheric holes made by ballistic missiles from North Korea detected with a Japanese dense GPS array, J. Geophys. Res., 115, A09314, doi:10.1029/2010JA015531, 2010.

Figure caption: TEC time series in the 2016 February launch of Kwangmyongsong-4 from North Korea are compared with the past three cases, i.e. the 1998 Taepodong-1, the 2009 Taepodong-2, and the 2012 Unha-3 launches. The 2016 case shows much larger TEC decreases than these past launches.

Keywords: GNSS-TEC, North Korean rocket, ionospheric hole

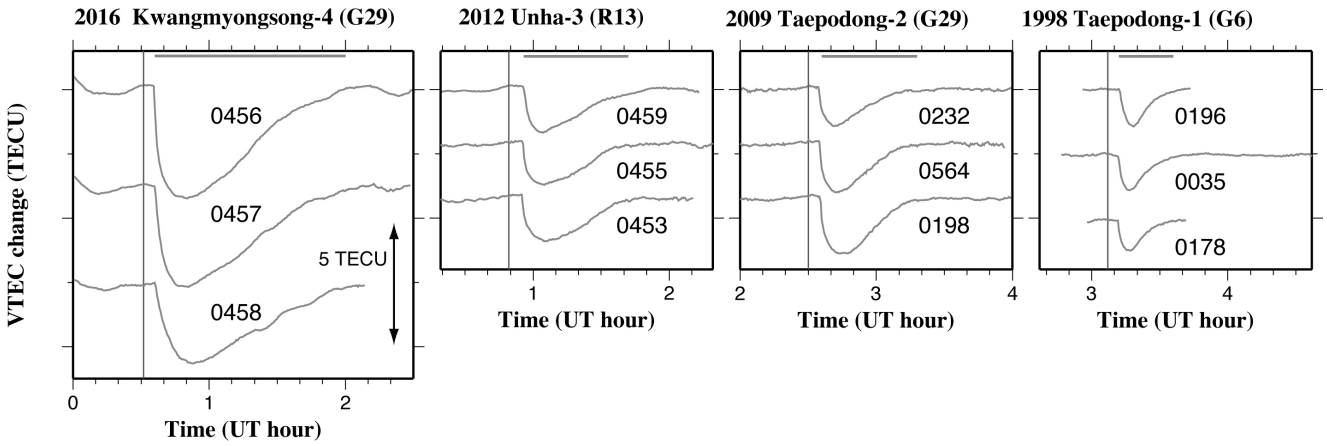

Analysis of Spatial Distributions of Total Electron Content Variations Associated with Earthquakes

*Shun Shomura[1], Hiroyuki Nakata[1], Hiroyo Ohya[1], Toshiaki Takano[1], Takuya Tsugawa[2], Michi Nishioka[2]

1.Graduate School of Engineering, Chiba University, 2.National Institute of Information and Communications Technology

It has been reported that ionospheric disturbances occur by giant earthquakes. This is because the acoustic wave and atmospheric gravity wave excited by ground perturbations or tsunami propagate into the ionosphere. Now that large-scale earthquake such as Tokai earthquake is predicted to occur, it is important to study ionospheric disturbances caused by the earthquake for revealing the mechanism of the earthquake.
In the previous studies, the variations of TEC associated with earthquakes have been confirmed by the frequency analysis of time-series data of total electron content (TEC) observed in Japanese GPS receiver net-work (GEONET). In this study, we have analyzed the spatial distribution of TEC variations in each directions of latitude and longitude by gaussian fitting. We examined the correlations of both spatial distributions of TEC variations and the magnitude. Ionospheric pierce points are assumed to be located at the height of the 350 km are determined. We calculated the spectral intensity in each frequency bands by the fast Fourier transform processing. We analyzed the 5 earthquakes of more than M6.8 that occurred around Japan since 2000.
As a result of the analysis, it is confirmed that the latitudinal distribution of TEC variations is highly correlated with the magnitude, while longitudinal one is not.

Keywords: Total electron content

The ionospheric variations associated with volcanic eruptions observed by GPS-TEC and HF Doppler

*Aritsugu Chonan[1], Hiroyuki Nakata[1], Hiroyo Ohya[1], Toshiaki Takano[1], Ichiro Tomizawa[2], Takuya Tsugawa[3], Michi Nishioka[3]

1.Graduate School of Engineering, Chiba University, 2.Center for Space Science snd Radio Engineering, 3.National Institute of Information and Communications Technology

It is reported that ionospheric disturbances are caused by ground and atmospheric perturbations, e.g. earthquakes and typhoons. Even though it is known that the volcanic eruptions excite the atmospheric waves, there are few observations of ionospheric disturbances caused by volcanic eruptions. In this study, we have examined ionospheric variations associated with volcanic eruptions using GPS-TEC and HF Doppler (HFD).

We analyzed TEC data observed by observed in GPS Earth Observation Network (GEONET) which is maintained by Geospatial Information Authority of Japan. Each pairs of satellites and receivers determines the value of TEC every 30 seconds. In this study, TEC data, in which mask angle is larger than 30 degrees, is used. We calculated the spectral intensity of TEC perturbations by Fast Fourier Transform (FFT). We analyzed 19 volcanic eruptions in Mts. Asama, Ontake and Shinmoedake since 2000. As a result, the variations of TEC by volcanic eruption are detected in 2 events. Both events are the eruptions in Mt. Asama with medium-size explosion. The center of the variations of TEC is located south of the volcano, which the same as the case for the earthquakes. Therefore the generation of the ionospheric perturbation associated with volcanic eruptions is the same process of that for the earthquakes. On the other hand, the variations of TEC at the frequency band of 7 ~ 12 mHz are shown, which is higher frequency than earthquakes.

We also analyzed HFD data transmitted from the Chofu campus of UEC for 4 events in Mt. Asama with medium-size explosion. We used the data observed at Sugadaira which is the nearest observation point from Mt. Asama. As a result, variations of TEC are detected in 3 events. In these events, the spectral intensity has peak a remarkable at 3 ~ 5 mHz and several peaks in 8 ~ 18 mHz. A peak at 3 ~ 5 mHz and 8 ~ 18 mHz are remarkable and there are a few peaks in the later. 3 ~ 5 mHz is due to acoustic resonance modes between the ground surface and the lower thermosphere as in variations of TEC associated with earthquakes. The perturbations around 8 ~ 18 mHz are also observed by GPS-TEC data, this caused that the pressure fluctuation excited by the explosion of the eruption directivity propagates to the upper ionosphere.

Keywords: ionosphere, volcanic eruptions

Seasonal variation in sunset ionospheric disturbances found in a long-term HF Doppler observation dataset

*Jun Sakai[1], Ichiro Tomizawa[1,2], Keisuke Hosokawa[2,1]

1.Center for Space Science and Radio Engineering, University of Electro-communications, 2.Department of Communication Engineering and Informatics, University of Electro-communications

Ionospheric disturbances are regularly observed after sunset. These disturbances can be associated with two major causes; on the one hand it is caused by the ionosphere itself with the elimination of ionization after sunset, on the other hand it is caused by atmospheric gravity waves (AGWs) which originate in lower atmosphere -presumably in the stratosphere or lower mesosphere -when the air becomes cold after sunset. These ionospheric disturbances are observed with radio instruments such as ionosondes, incoherent scatter radars, HF Doppler (HFD), and GPS TEC. However, except for HFD, it is inherently difficult to identify the causes of the disturbance from data obtained by these methods. Recently, by employing HFD, one of the authors and his colleague identified the altitude of the source region of an AGW which caused an ionospheric disturbance after sunset; it is suggested that the source altitude was about 50 km, which roughly corresponds to the upper bound of the ozone layer. As a sunset is a regular periodic phenomenon, the seasonal variations of the ionospheric disturbances associated with a sunset can be isolated from others relatively easily. It is therefore useful to study ionospheric disturbances after sunset to understand the characteristics of atmosphere-ionosphere coupling. In this study, we present some features of seasonal variation in sunset ionospheric disturbance obtained from a long-term HFD dataset.

Keywords: ionospheric disturbance, sunset, HF Doppler

Improvement of the electron density automatic estimation algorithm in the ionosphere lower region

*Ryota Nakazawa[1], Taketoshi Miyake[1], Keigo Ishisaka[1]

1.Toyama Prefectural University

In the lower ionosphere, the approximate electron density profile can be estimated from the comparison between these observation results obtained by sounding rocket and propagation caracteristics calculated with Full wave method. This estimation process, which is so-called ”wave absorption method”, has some problems. At first, we have no clear standard for comparing observation results and propagation characteristics calculated with Full wave method. In addition, we have to iterate many times correcting the electron density profile by handwork, calculating propagation characteristics with Full wave method and comparing observation results and calculated propagation characteristics. This iteration takes too long to estimate appropriate electron density profile. To reduce these problems, we developed an application to realize automated estimation of electron density profile by analyzing radio wave propagation characteristics.
In the past of the research, they were estimated electron density by automated estimate application. In the result, I realized high accuracy estimation because error was within 1.2 dB in all estimated area. And it can estimate at short time. However there was a large fluctuation of the electron density in low-altitude part. This is impossible in actual observation. So, we did consideration and improvement to algorithm.

Keywords: ionosphere, plasma waves, electron density profile, Full wave method

Rocket GPS-TEC Tomography method to obtain high altitude resolution

*Yutaro Ikehata[1], Yuki Ashihara[1]

1.Department of Electric and Information Engineering National Institute of Technology, Nara College

In the high altitude atmosphere of the earth, there is a layer of atmosphere called ionosphere, filled with extricated electrons, and the observation of the electron density profile in the ionosphere is recently taken notice of.
As an approach to the observation of electron density profile in the ionosphere, there is the remote sensing method called GPS-TEC method, which calculates the total electron counts (TEC) on the transmission path of GPS wave, from its propagation delay. By applying tomography analysis on TEC values in multiple paths, which are one dimensional information, the electron distribution profile can be earned as two dimensional data, and this method is called GPS-TEC tomography method. However, this method has a defect, that it has low resolution in altitude direction.
In order to enhance the altitude resolution, we have proposed “Rocket GPS-TEC Tomography method,” which applies tomography analysis on the TEC values earned by rocket observation. Compared to the conventional GPS-TEC tomography, this method can observe TEC values in horizontal paths, as the observation rocket navigates in both range and altitude direction. By this approach, we assumed that altitude resolution of the tomography result will improve. In this study, we verified the efficacy of proposed method through simulation experiment.

Keywords: ionosphere, GPS-TEC, sounding rocket

Effect of intrinsic magnetic field decrease on the low-to-middle latitude ionosphere-thermosphere dynamics simulated by GAIA

*Chihiro Tao[1], Hidekatsu Jin[1], Hiroyuki Shinagawa[1], Hitoshi Fujiwara[2], Yasunobu Miyoshi[3]

1.National Institute of Information and Communications Technology, 2.Seikei University, 3.Kyushu University

The Earth's intrinsic magnetic field has been fluctuated between 10^{22}-10^{23} Am^2 in past 0.8 million years and now under decreases at a rate of ~6% per century. The intrinsic field decrease would modify not only the ionosphere via electromagnetics, but also the atmosphere under interactions with the ionosphere. The relationship between long-term variations of observed Sq field and the intrinsic magnetic field has evaluated by simulation studies. Cooling of the upper atmosphere observed over past decades is also suggested to be contributed by the intrinsic field variation in addition to the effect by CO_2 enhancement in the low altitude. The upper atmosphere dynamics is largely affected by the lower atmosphere. This study investigates the effect of intrinsic magnetic field on the coupled system using a numerical model, GAIA (Ground-to-Topside Model of Atmosphere and Ionosphere for Aeronomy), which solves physical and chemical dynamics of the whole atmosphere region from troposphere to exosphere under interaction with the ionosphere.
The model simulation is operated with a reduced (50% and 75%) intrinsic magnetic field referring to February 2008 when the wave-4 structure is appeared and solar activity was quiet. In order to focus on the low-to-middle latitude profiles, this experiment excludes the cross-polar cap potential and auroral electron input.
The calculated parameters averaged over the 250 km shows small variations in the neutral wind velocity and electron density with magnetic field changes, while the dynamo electric field decreases and the ionospheric horizontal current increases with increasing magnetic field. In addition to the proportional dependence of the dynamo field on the magnetic field, the ionospheric conductance dependence with $\sim B^{-2\sim-1}$ due to an upward shift of the conductance shift affects the horizontal current. The decreased magnetic field provides the zonal wind enhancement and upward shift of electron peak altitude in the equatorial region. We will report the cause of these variations and their effects on the wave propagation.

Keywords: thermosphere-ionosphere, low-to-middle latitude, intrinsic magnetic field dependence

Horizontal structures of Helium ion in the upper ionosphere observed by ISS-IMAP/EUVI

*Yuta Hozumi[1], Akinori Saito[1], Ichiro Yoshikawa[2], Atsushi Yamazaki[3], Go Murakami[3]

1.Graduate School of Science, Kyoto University, 2.The University of Tokyo, 3.Institute of Space and Astronautical Science / Japan Aerospace Exploration Agency

Horizontal structures of ionized Helium in the upper ionosphere of dusk side were obtained from observation of resonant scattering light. The Extreme Ultra Violet Imager (EUVI) of the ISS-IMAP (Ionosphere, Mesosphere, upper Atmosphere and Plasmasphere mapping) mission has taken image of He II radiation (30.4 nm) from the International Space Station (ISS) since October 2012. North-south asymmetry and longitudinal structure of ionized Helium were found. North-south asymmetry in solstice seasons are well consistent with previous in-situ measurement and numerical simulation. However, the longitudinal structure is not reported before and cannot be explained by numerical simulation with SAMI2-model. The longitudinal difference of meridional wind is a candidate of the Helium ion structure.

Ionospheric Scintillation Observations with GNSS receivers in Tromsoe, Norway

*Yuichi Otsuka[1], Kodai Uwashitomi[1], Yasunobu Ogawa[2], Keisuke Hosokawa[3]

1.Institute for Space-Earth Environmental Research, Nagoya University, 2.National Institute of Polar Research, 3.University of Electro-Communications

Ionospheric scintillation is a phenomenon that received radio wave fluctuates in phase and amplitude. We have been operating dual-frequency GNSS (Global Navigation Satellite System) receivers at Tromsoe, Norway to measure signal intensity and phase of the radio waves at a sampling rate of 50 Hz.
We have analyzed ROTI, defined as a standard deviation of the differential of TEC (Total Electron Content) during 1 minutes. At 00:10-00:20 UT on 8 Februay 2014, ROTI increased to 0.7 TECU/min, but S4 did not increase. We have calculated cross-correlation coefficient (CCC) of TEC variation obtained at two-antennas installed with a mutual distance of 242 m, and found that CCC is close to unity. This result indicate that the plasma density in the ionosphere is spatially homogeneous although it varies temporally. On the other hand, at 11:30-12:00 UT on 27 October 2014, S4 index increased to 0.4 whereas ROTI was low. For this event CCF of TEC variations at the two-antenna is approximately 0.6, indicating the ionospheric plasma density was inhomogeneous to cause amplitude scintillation.

Keywords: ionosphere, GNSS, scintillation

